Environmental Science Nano

Nano-QSAR modeling for ecosafe design of second generation TiO_2-based nano-photocatalysts

Journal:	*Environmental Science: Nano*
Manuscript ID	EN-ART-01-2018-000085.R1
Article Type:	Paper
Date Submitted by the Author:	26-Feb-2018

Complete List of Authors:	Mikolajczyk, Alicja; University of Gdansk, Faculty of Chemistry Gajewicz, Agnieszka; Univesity of Gdańsk, Departmnet of Chemistry Mulkiewicz, Ewa; University of Gdansk, Department of Environmental Analytics, Faculty of Chemistry Rasulev, Bakhtiyor; North Dakota State University, Department of Coatings and Polymeric Materials Marchelek, Martyna; University of Gdansk, Department of Environmental Technology Diak, Magdalena; Faculty of Chemistry, University of Gdansk, Department of Environmental Technology Hirano, Seishiro; National Institute for Environmental Studies, RCER Zaleska-Medynska, Adriana; University of Gdansk, Department of Environmental Technology Puzyn, Tomasz; University of Gdansk, Laboratory of Environmental Chemometrics, Faculty of Chemistry

Due to their extraordinary properties, new surface modified nanoparticles (so-called *second generation* of NPs) offer promising avenues for future innovation, e.g. as environmentally friendly photocatalyst that promote degradation of a variety of organic and inorganic compounds. However, modification, and in result, obtained physicochemical properties that make the second generation NPs of great industrial interest may also endanger human health through the potential quick distribution in environment and following induction of cytogenetic, mutagenic and/or carcinogenic effects. Therefore, in light of the increasing number of newly synthetized heterogeneous nanoparticles, and the serious health risk that they may cause, the development of new methods for quantifying environmental health risks is paramount.

Journal Name

ARTICLE

Nano-QSAR modeling for ecosafe design of second generation TiO_2-based nano-photocatalysts

Received 00th January 20xx,
Accepted 00th January 20xx

DOI: 10.1039/x0xx00000x

www.rsc.org/

Alicja Mikolajczyk[a,b], Agnieszka Gajewicz[a]*, Ewa Mulkiewicz[c], Bakhtiyor Rasulev[d], Martyna Marchelek[b], Magdalena Diak[b], Seishiro Hirano[e], Adriana Zaleska-Medynska[b] and Tomasz Puzyn[a]

The human health and environmental risk assessment of engineered nanomaterials (NPs) is nowadays of high interest. It is important to assess and predict biological activity, toxicity, physicochemical properties, fate and transport of NPs. In this work combined experimental and computational study is performed in order to estimate toxicity and develop a predictive model for heterogenous NPs (i.e. modified NP, created by more than one type of NPs). Quantitative structure-activity relationship (QSAR) methods have not been yet adopted for predicting the toxicity/physicochemical properties of modified heterogeneous nanoparticles (so-called second generation NPs). Since the main problem for Nano-QSAR/Nano-QSPR modeling of second generation NPs was a lack of appropriate descriptors that able to express the specific characteristics of 2nd generation NPs we developed here a novel approach. The novel approach to encode heterogenous NPs is based on idea of additive descriptors for mixture systems previously applied only for mixture of organic/inorganic compounds. Thus, based on proposed novel approach we have performed experimental and theoretical studies to develop Nano-QSAR models describing the cytotoxicity of 34 TiO_2-based NPs modified by (poly-)metallic clusters (Au, Ag, Pt) to the Chinese hamster ovary cell line. The models showed a good predictive ability and robustness. This approach can be used as an efficient tool for assessing the toxicity as well as physicochemical properties of unexplored 2nd generation NPs.

1. Introduction

Pristine metal oxide nanoparticles (so-called first generation NPs) represent one of the most important groups of NPs because of their remarkable mechanical, electronic, magnetic, catalytic and photocatalytic properties. Due to the number of applications in various segments, metal oxide nanoparticles are accounted for the largest share of the total nanoparticles market in 2015.[1] The analysts forecast a global metal oxide nanoparticles market to grow at a CAGR (Compound Annual Growth Rate) of 9.5% during the period 2016-2020, likely rising to almost 2 million tons by 2020.[1] Therefore, it is necessary to develop new methods allowing for quick assessment of their toxicity and fate in the environment. Since their extraordinary properties, metal oxide based composite nanoparticles (so-called second generation nanoparticles, e.g. $Me_{mix}@MeO_x$, where Me_{mix} is a bimetallic cluster, MeO_x is metal oxide nanoparticle) may serve as environmentally friendly photocatalysts that promote degradation of a variety of organic and inorganic compounds.[2, 3] Those types of nanoparticles could be used for visible light induced processes to remove harmful pollutants from gas and aqueous phases.[2, 4] However, modification, and in result, obtained physicochemical properties that make the second generation nanoparticles ($Me_{mix}@MeO_x$) of great industrial interest may also result in potential risks to human health and environment.[5, 6] Recent publications report the numerous evidences for (eco)toxicity of engineered nanomaterials highlighting the potential risk related to the development of nanotechnologies.[7] The conventional (i.e. experimental) risk assessment approaches are often expensive, time-consuming and inadequate for enabling safety precautions for newly developed materials in the fast moving market of NPs. Thus, development of computationally-based assessment methods complimentary to experiments is will allow to reduce the number of experiments and the amount of consumables reagents. One of the most promising approaches that can be applied for this purpose is a Quantitative Structure-Activity Relationship (QSAR) approach, which was offered for the first time in 1962 by Corwin Hansch and then implemented in development of new chemicals, mainly drugs.[8] A relatively

[a] Laboratory of Environmental Chemometrics, Faculty of Chemistry, University of Gdansk, Wita Stwosza 63, 80-308 Gdansk, Poland. E-mail: a.gajewicz@qsar.eu.org.
[b] Department of Environmental Technology, Faculty of Chemistry, University of Gdansk, Wita Stwosza 63, 80-308 Gdansk, Poland.
[c] Department of Environmental Analytics, Faculty of Chemistry, University of Gdansk, Wita Stwosza 63, 80-308 Gdansk, Poland.
[d] Center for Computationally Assisted Science and Technology, North Dakota State University, NDSU Research Park Drive, P.O. Box 6050, Fargo, North Dakota 58108, United States
[e] Center for Environmental Risk Research, National Institute for Environmental Studies, Tsukuba, 16-2 Onogawa, Ibaraki 305-8506, Japan
† Footnotes relating to the title and/or authors should appear here.
Electronic Supplementary Information (ESI) available: [details of any supplementary information available should be included here]. See DOI: 10.1039/x0xx00000x

newly developed type of QSAR methodology, QSAR for nanoparticles or Nano-QSAR, is based on defining mathematical dependencies between the variance in molecular properties, encoded by so-called 'nano-descriptors' and the variance in biological activity for a set of nanomaterials.[9-11] This means, if one has calculated or experimentally measured properties (descriptors) for a group of similar nanomaterials and the toxicological data are available only for a part of this group, one is able to predict the missing data from the theoretically-generated descriptors and a developed mathematical QSAR model. It is interesting to mention that "intelligent" consensus modelling approach integrating individual models derived using different combination of descriptors and/or different modelling methods have received a lot of attention over the past several years.[9-10] As recently pointed out by Roy et al.,[9] consensus models improve the predictability, due to the fact that prediction of query compounds can rely on multiple individual models instead of single QSAR model prediction. The successful concept and application of Nano-QSAR/QSPR and consensus modelling approach have been already demonstrated, but only for simple, so-called 1st generation NPs, such as: metal oxides, silver clusters, carbon nanotubes and fullerenes.[11-29] Unfortunately, until now, there were no suitable and reliable approaches to calculate nano-descriptors for the 2nd generation of Me_{mix}@MeOx NPs, therefore no Nano-QSAR/QSPR models were dedicated for such type of NPs. Since the 2nd generation NPs share properties associated with both solutes and separate particle phases they have higher degree of complexity and multi-functionality in comparison to 1st generation NPs.[24] Thus, more sophisticated approaches to calculate nano-descriptors, i.e. specific properties that able to assess the activity of such NPs are needed.

The aim of this study is to develop an approach for nanodescriptors generation which are able to characterize the 2nd generation photocatalytic NPs. In view of this, a series of noble metal surface decorated TiO_2-based photocatalysts differing type and amount of metals immobilized at the surface of TiO_2 has been investigated, both experimentally and theoretically. In this work we have proposed to extend the idea of additive descriptors for mixture, previously applied only for mixtures of organic compounds[30-42] to the 2nd generation NPs. Finally, we have demonstrated the usefulness of the proposed approach in describing the unique physicochemical and electronic properties of 2nd generation NPs. The combined experimental and theoretical study allowed us to develop interpretative Nano-$QSAR_{mix}$ models for toxicity of 34 TiO_2 NPs modified by mono or bimetallic clusters (Au, Ag, Pt) to Chinese hamster ovary (CHO) cells. In result, we have defined a number of structural features of investigated Me_{mix}@TiO_2 NPs that have the highest influence on observed cytotoxic effect.

1.1 General approach: How to perform modeling of mixture systems?

For the mixtures of conventional organic compounds four major types of modes of action were previously defined: (i) simply additive, i.e. ideal additive effects are observed when the joint toxic response is equal to a sum of the single chemical toxicity, (ii) more than additive/synergism, i.e. combined effect is greater than a sum of the toxicity of individual chemical, (iii) less-than-additive/partial addition, i.e. overall toxic effect is less than a sum of the toxicity of individual chemical, (iv) no interaction/independent, i.e. joint toxic effect is equal to that caused by the component with the greatest toxicity.[34, 38] According to the results reported in the literature, the simple additivity scheme is appropriate for preliminary modeling of toxicity of multiple chemicals' mixtures.[38] Moreover, based on detailed reviewing the results in previous studies it can be seen that the joint effects of non-reactive chemicals are not significantly different from the simple addition scheme. As such, we have decided to explore additive mixture descriptors to describe the 2nd generation TiO_2-based NPs. For this purpose, we have assumed that each individual component affects the toxicity of a mixture additively and its contribution is proportional to the mole fraction of the individual constituents in the mixture.[34-38] Thus, doses/concentrations of the single components in a mixture are added after being multiplied by a scaling factor (a) that accounts for the property contribution of the individual component. The mixture-based property of the NP (C_{mix}) is the sum of the doses/concentrations (a) of the individual components C_i (eq. 1):

$$C_{mix} = \sum_{i=1}^{n} aC_i \quad (1)$$

Although the above-mentioned descriptors are widely used in QSAR studies for conventional organic chemical mixtures[39-46], there are no examples of successful application of integral additive descriptors to describe the property of a mixture of NPs or complex/composite NPs. In this study we have proposed the adaptation of the methodology of integral additive descriptors for conventional mixture systems that have proved their usefulness in the past to 2nd generation NPs. Thus, we have employed the integral additive descriptors approach to describe the influence of the type and amount of noble-metal precursor on the structure of 2nd generation NPs.

For example, Wang *et al.*[47] used this type of approach to describe the *n*-octanol/water partition coefficient for binary mixture ($\log P_{mix}$) based on *n*-octanol/water partition coefficient for a single compound ($\log P$) described by eq. 2:

$$\log P_{mix} = (C_A \times \log P_A + C_B \times \log P_B + \ldots) / (C_A + C_B + \ldots) \quad (2)$$

where: $\log P_A$ and $\log P_B$ are *n*-octanol/water partition coefficients of components A and B respectively, C_A and C_B are

the concentrations of components A and B, respectively, in binary mixtures.

Thus, in the framework of integral additive descriptors any individual compound can be expressed by a set of various 2D and 3D descriptors. For example, Todeschini and Consonni[48] described useful 2D and 3D descriptors that can be calculated by Dragon and Gaussian software.[48, 49] Then descriptors of mixture system can be expressed as a mole weighted average using the calculated descriptor(s) value(s) and mole fraction of each component as follow[35] (eq. 3)

$$D_{mix} = R_1D_1 + R_nD_n \quad (3)$$

where: D_{mix} is the mixture descriptor, R_1 and R_n are the mole fractions of the components in the mixture, and D_1 and D_n are the descriptors of each of component in the mixture.

2. Materials & methods

2.1 Set of second generation NPs

In this study, a set of 34 TiO_2 NPs modified with different type and amount of noble metals (mixture of Ag, Au, Pt) is investigated. All studied NPs were obtained by microemulsion method. The technical details regarding the experimental conditions, such as materials synthesis, preparations of modified TiO_2 nanostructures, characterization, are listed in Supplementary information (Tables S1 and S2).

2.2 Empirical toxicity testing

The cytotoxicity of the $Me_{mix}@TiO_2$ was experimentally tested using Chinese hamster ovary (CHO-K1, ATCC® CCL-61™) cell line. For the experiment, investigated nanomaterials have been prepared by grinding the powder for 5 min, then dissolved in a cell medium to a concentration of 1 mg/ml (F12 medium supplemented with 2 mM l-glutamine, 1% antibiotic solution (penicillin/streptomycin) and 10% FBS Hi) with 0.1% Pluronic added to prevent aggregation/agglomeration, and then sonicated in a water bath for 30 min at 37 °C. A colorimetric assay with WST-8 reagent was used for the cell viability tests. For the assays, cells were seeded in 24-well plates at an initial density of 1×10^5 cells/ml of culture medium and incubated for 24 h. Cells were exposed to nine different concentrations of NPs (from 300 to 1.56 μg/ml) for 24 h. Subsequently, WST-8 reagent was added to each well and incubated for 2 h. Because Au NPs absorb light in the visible spectrum, the plates were centrifuged to avoid interference with the assay. Subsequently, 100 μl of medium from each well was transferred to a respective well in a 96-well plate and the absorbance at 450 nm was measured in the plate reader. Cell viability was calculated as the percentage of the viability of exposed cells vs. controls. Concentration-response curves were fitted using the nonlinear least-squares method employing the logistic model of the relation between cell viability and the tested concentrations. Obtained EC_{50} value is the concentration of NP that causes a 50% inhibition of the cell viability. The EC_{50} values were converted to the $\log(EC_{50})^{-1}$ values for further nanostructure-activity relationship modeling. Calculations were carried out with the R programming language and environment for statistical computing (http://www.r-project.org).

2.3 Quantum–mechanical calculations

In order to investigate modified TiO_2-based NPs and identify the structural features responsible for their biological activity (i.e. toxicity to CHO cells), we have calculated quantum-mechanical (QM) descriptors in addition to additive descriptors discussed above. For this purpose, a number of QM properties quantitatively describing the particular variability of the structural features of $Me_{mix}@TiO_2$ were calculated. The calculations were performed at the Density Functional Theory (DFT) level with use of B3LYP functional and LANL2DZ basis set in Gaussian 09 software package, as well as application of Vienna *ab-initio* Simulation Package (VASP).[49, 50] The calculations were conducted as a two-step protocol including: (i) investigation of metal clusters in a gas phase, at *B3LYP/LANL2DZ* level and (ii) solid state systems of $Me/Me_{mix}@TiO_2$, using the plane-wave based method in VASP, implementing spin-polarized DFT and the generalized gradient approximation (GGA) by Perdew-Burke-Ernzerhof (PBE) with an intra-site Coulomb interactions between Ti-3d electrons in Dudarev's approach; so-called PBE+*U*.51 The core electrons for Au-[Xe]$4f^{14}$, O-$1s^2$ and Ti-[Ne]$3s^2$ were described by projector augmented wave potential (PAW).[51-54] As a result: energy of highest occupied molecular orbital (E_{HOMO}); energy of lowest unoccupied molecular orbital (E_{LUMO}); ionization potential (I); electron affinity (A); absolute electronegativity (μ); absolute hardness (η); total energy of the system (E_{tot}) and adsorption energy of metal (E_{ads}) were calculated and applied in further steps (Table 1).

Table 1. Description of selected descriptors used in presented study.[34]

Descriptor	Formula	Description
ionization potential	$I = E_C^{N-1} - E_0^N$	E_C^{N-1} is the energy after losing one electron (cation) E_0^N is the basal state energy (neutral)
electron affinity	$A = E_0^N - E_A^{N+1}$	E_A^{N+1} is the energy after gaining one electron (anion)
absolute electronegativity	$\mu = \frac{(I + A)}{2}$	μ is absolute electronegativity, I is ionization potential, cation electronegativity
absolute hardness	$\eta = \frac{(I - A)}{2}$	η is absolute hardness, A is electron affinity
adsorption energy of metal	$\Delta E_{ads} = E_{tot} - (E_{TiO_2} + E_{Me})$	E_{tot} is the total energy of the interacting metal with TiO_2 surface; E_{TiO_2} is the total energy of the clean most stable TiO_2; E_{Me} is the total energy of the single metal atom

As stated above, the conventional descriptors derived from quantum-mechanical calculations (Table 1) can be adapted to calculate integral additive descriptors for surface-modified metal oxide nanoparticles (i.e. 2nd generation NPs). Thus, in order to reflect the molecular structure of 2nd generation NPs with various modifications such as: a variety of concentrations of single metal cluster, different type and amount of noble-metal precursor on the surface of TiO_2-based NPs we have proposed the application of a modified form of the Eq. 3. The proposed mixture descriptor calculation methodology can be described by the following equation (Eq. 4):

$$D_{mix} = \%mol_{Me_1} \times F_1 + \ldots + \%mol_{Me_n} \times F_n \quad (4)$$

where: D_{mix} is the mixture descriptor, i.e. the information on structure features of NP component translated into numerical variables; $mix\ \%mol_{Me_n}$ is a certain feature, i.e. concentration of each metal/component in mixture – contribution by weight of metal in NP sample of mixture; F_n is a quantum mechanical descriptor for the certain metal/component.

Proposed methodology is based on the abovementioned assumption that 2nd generation NP can be represented as a mixture system of individual metals in the clusters (fragment representation). Each metal can be described by a set of descriptors, i.e. numerical characteristics of the molecular representation calculated from e.g. quantum-mechanical calculations. Then computed properties (i.e. descriptors) of each metal (Me) that result from the high-level quantum-mechanical calculations are multiplied in a proportion to the amount of metal within the mixture (Me_{mix}). The sum of resulting values represents a new descriptor of a complex system. The methodology for computing of integral additive descriptors is graphically presented in Figure 1. Finally, to illustrate the usefulness and the effectiveness of the proposed approach with use of the additive descriptors for 2nd generation NPs (eq. 4) the Nano-QSAR$_{mix}$ models predicting the toxicity of 34 TiO_2-based NPs modified by (poly-)metallic clusters (Au, Ag, Pt) to the Chinese hamster ovary cells have been developed and validated.

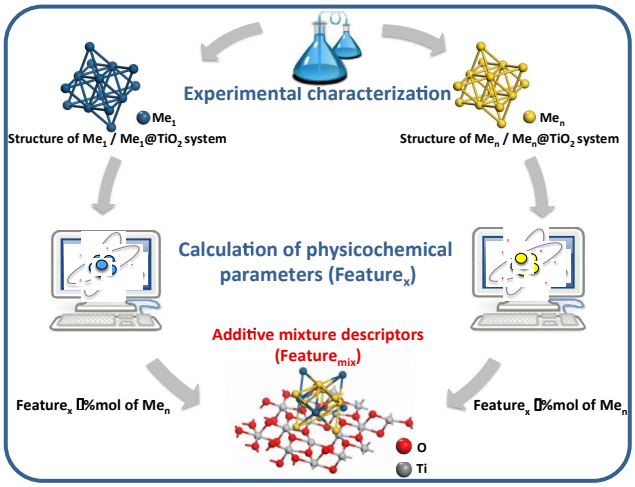

Figure 1. The overall scheme of calculating the additive descriptors for mixtures.

2.4 Data splitting for Nano-QSAR modeling

The nanoparticles of $Me_{mix}@TiO_2$ NPs for which the experimental data have been measured were divided into two sets: the training set (T, to develop a Nano-QSAR$_{mix}$ model) and validation set (V, to validate the model's predictive ability), to guarantee a balanced distribution of compounds covering the whole range of cytotoxicity to both training and validation sets. For this, an effective algorithm of splitting, so-called 'X:1'[56], where X=4 was applied. By using 'three-to-one' algorithm of splitting we have obtained the following: training set (containing 76% of all $Me_{mix}@TiO_2$ NPs) and validation set (containing 24% of all $Me_{mix}@TiO_2$ NPs). For more details please refer to SI (Table S3).

2.5 Multiple Linear Regression analysis (MLR) and Nano-QSAR approach

In order to develop a Nano-QSAR$_{mix}$ model the Multiple Linear Regression (MLR) technique was employed. MLR is a commonly used statistical tool where dependent variable (e.g. toxicity ($\boldsymbol{y}_i$)) is expressed as a linear combination of the independent variables (e.g. physicochemical properties and/or structural features ($\mathbf{x_1}$, $\mathbf{x_2}$, … , $\mathbf{x_n}$)) (eq. 5). The most relevant subset of physically interpretable independent variables (i.e. molecular descriptors) was selected using genetic algorithm (GA), implemented in QSARINS software.[52]

$$\mathbf{y}_i = \mathrm{b}_0 + \mathrm{b}_1\mathbf{x}_1 + \mathrm{b}_2\mathbf{x}_2 + \cdots + \mathrm{b}_n\mathbf{x}_n \quad (5)$$

The Nano-QSAR$_{mix}$ model has been developed according to the golden standards and recommendations of the Organization for Economic Co-operation and Development (OECD).[58] Goodness-of-fit was accomplished by calculating the determination coefficient (R^2) and the root mean square error of calibration ($RMSE_C$) based on the prediction for the training set. Model's robustness, which describes the stability of its parameters for deletion of one or more compounds, was verified by performing the internal validation with cross-validation Leave One Out (LOO) algorithm. The robustness of the model was expressed by the cross-validation coefficient (Q^2_{CV}) and the root mean square of cross-validation ($RMSE_{CV}$). Developed model's predictive ability was assessed by calculating: the external validation coefficient (Q^2_{Ext}), root mean square error of prediction ($RMSE_P$), Concordance Correlation Coefficient (CCC), accuracy and different variants of r^2_m.[42-43, 59-62] In addition, the model's predictive power was examined by applying the statistical tests for the continuous predictive models. It is worth to highlight that both internal and external validation were performed according to the rigorous criteria formulated by Golbraikh and Tropsha[42-44] (for more details please refer to Supplementary information: Table S4, Table S9).

In order to avoid any bias in descriptor selection the double cross-validation approach was additionally used.[45] The GA-MLR model development using the double cross-validation process has been performed with the *Double Cross-Validation Tool*

(version 2.0) developed by Roy and Ambure.[45] The statistical metrics used to characterize the internal and external validation of the final Nano-QSAR models are reported in Supplementary Information, Table S8. In addition, the applicability domain (AD) that shows the virtual space in which the model can make predictions with the optimal reliability has to be assessed. In the presented work the Williams plot was used to assess applicability domain (AD) of the final developed model (for more details please refer to Supplementary information, Table S5).

3. Results and discussion

In recent paper[2] we published results that demonstrate potential application of surface modified TiO_2 NPs as photocatalyst for degradation of pollutants. However, the same modification that influences photocatalytic properties of TiO_2-based NPs can results in unknown risk to human body and the environment. Therefor based on developed approach and experimentally determined toxicity effect (EC_{50}) of 34 TiO_2-based NPs to Chinese hamster ovary cells (Table 2) we described properties that can influence potential hazardous of designed heterogeneous photocatalysts. In the next step, the changes in the cytotoxicity values depending on the type and amount of selected noble metals on the surface of TiO_2 were qualitatively investigated by applying visualization techniques (i.e. heatmaps). Results obtained by analyzing Figure 2 revealed pronounced trends (i.e. systematic patterns). We have found that with increasing amount of silver metal on the surface of TiO_2 the toxicity of NPs to CHO cells increases. This observation is obvious in the light of previous contributions,[65-68] however, it needs to be emphasized that for the other noble metals similar trends have not been observed.

By applying the proposed methodology for computing the additive descriptors for 2nd generation NPs (eq. 4) we have calculated a set of nine mixture descriptors reflecting the properties of 34 of TiO_2-based NPs. The computed values of all descriptors are presented in Table S6 (for more details please refer to Supplementary information Table S6).

Finally, by combining the experimental and theoretical study (i.e. cytotoxicity data obtained for CHO-K1 cell line and selected novel additive structural descriptors for Me_{mix}@TiO_2 NPs) we have developed two types of the statistically significant Nano-$QSAR_{mix}$ models that reliably predict the toxicity of all considered compounds. Each established Nano-$QSAR_{mix}$ model has utilized only one descriptor. The first Nano-$QSAR_{mix}$ model, so-called metal concentration-based model employs as independent variable the amount of silver metal precursor in a mixture (%mol_{Ag}, eq. 6), while the second one, so-called mechanistically-based Nano-$QSAR_{mix}$ model, uses as descriptor the absolute electronegativity of the whole mixture system (μ_{mix}, eq. 7). Following the OECD QSAR validation recommendations[58, 60] both Nano-$QSAR_{mix}$ models have been validated (internally and externally).

Table 2. Summary of experimental data that characterize modified TiO_2 samples prepared by microemulsion method in this study.

Sample	Amount of noble metal precursor [mol %]			Toxicity $log(EC_{50})^{-1}$ [molar]
	Ag	Pt	Au	
Pure TiO_2	0	0	0	4.43
0.1Pt	0	0.1	0	4.53
0.1Au	0	0	0.1	4.56
0.25Au	0	0	0.2	4.62
0.5Ag_0.1Pt	0.5	0.1	0	4.64
0.25Au_0.25Pt	0	0.25	0.2	4.66
0.05Au_0.05Pt	0	0.05	0.0	4.67
0.25Pt	0	0.25	0	4.67
0.5Au_0.5Pt	0	0.5	0.5	4.68
0.1Au_0.1Pt	0	0.1	0.1	4.68
0.5Au_0.25Pt	0	0.25	0.5	4.70
0.1Au_0.25Pt	0	0.25	0.1	4.70
1.25Pt	0	1.25	0	4.71
0.5Ag	0.5	0	0	4.72
0.5Pt	0	0.5	0	4.73
0.5Ag_0.25Pt	0.5	0.25	0	4.73
0.5Au_0.1Pt	0	0.1	0.5	4.75
0.25Au_0.1Pt	0	0.1	0.2	4.76
1.5Ag_0.1Pt	1.5	0.1	0	4.84
1.5Ag	1.5	0	0	4.89
0.5Ag_0.5Pt	0.5	0.5	0	4.94
1.5Ag_0.25Pt	1.5	0.25	0	5.01
2.5Ag_0.1Pt	2.5	0.1	0	5.06
1.5Ag_0.5Pt	1.5	0.5	0	5.26
2.5Ag_0.5Pt	2.5	0.5	0	5.32
2.5Ag	2.5	0	0	5.35
2.5Ag_0.25Pt	2.5	0.25	0	5.37
4.5Ag_0.1Pt	4.5	0.1	0	5.54
6.5Ag_0.1Pt	6.5	0.1	0	5.63
4.5Ag_0.25Pt	4.5	0.25	0	5.65
4.5Ag_0.5Pt	4.5	0.5	0	5.65
4.5Ag	4.5	0	0	5.70
6.5Ag_0.5Pt	6.5	0.5	0	5.80
6.5Ag_0.25Pt	6.5	0.25	0	5.84
6.5Ag	6.5	0	0	5.88

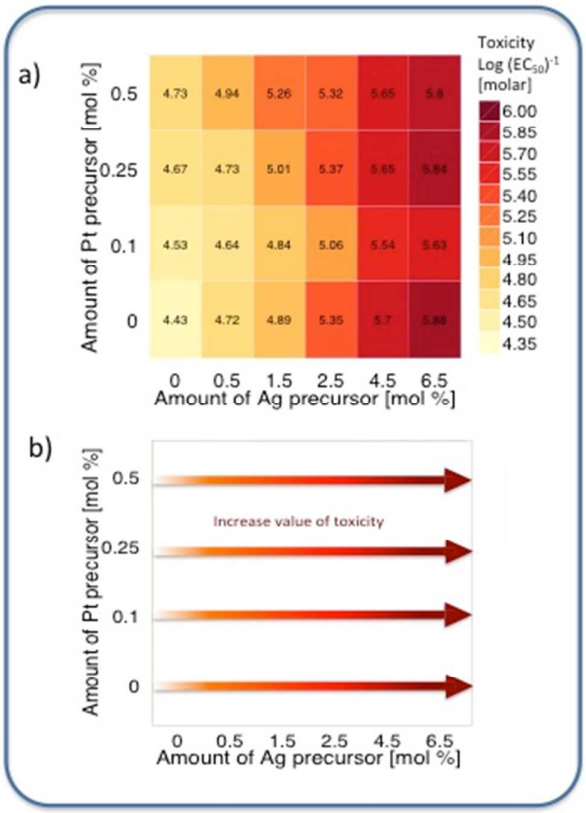

Figure 2. (a) The relationship between the cytotoxicity and amount of selected noble metals on the surface of TiO_2 and (b) a tendency of Ag metal precursor distribution towards increasing cytotoxicity effect [%]. Colors represent the logarithmic values of the cytotoxicity to Chinese hamster ovary cell line: yellow color means the lowest value of a given endpoint (4.35 value on the scale), whereas red color represents the highest values of a studied cytotoxicity.

The following equations Eq.6 and Eq.7 are developed:

$$\log(EC_{50})^{-1} = 4.6943 + 0.1822\%mol_{Ag} \quad (6)$$

n=26, k=8, R^2=0.93, R^2_{adj}=0.93, R^2-R^2_{adj}=0.00, Q^2_{LOO}=0.92, R^2_{Ext}=0.90, Q^2_{F1}=0.88, Q^2_{F2}=0.88, Q^2_{F3}=0.90, CCC_{Ext}=0.93, r^2_m=0.74, k=1.01, k´=1.00, $RMSE_C$=0.11, $RMSE_{CV}$=0.13, $RMSE_P$=0.14, s=0.12, F=340.82

where: $\%mol_{Ag}$ is the amount of silver metal precursor in a mixture.

$$\log(EC_{50})^{-1} = 4.6275 + 0.0004\mu_{mix} \quad (7)$$

n=26, k=8, R^2=0.94, R^2_{adj}=0.94, R^2-R^2_{adj}=0.00, Q^2_{LOO}=0.93, R^2_{Ext}=0.90, Q^2_{F1}=0.83, Q^2_{F2}=0.83, Q^2_{F3}=0.87, CCC_{Ext}=0.89, r^2_m=0.56, k=1.00, k´=1.00, $RMSE_C$=0.11, $RMSE_{CV}$=0.12, $RMSE_P$=0.16, s=0.11, F=384.32

where: μ_{mix} is absolute electronegativity of the mixture system investigated, developed based on the following equation:

$$\mu_{mix} = \%mol_{Ag} \times \mu_{Ag} + \%mol_{Au} \times \mu_{Au} + \%mol_{Pt} \times \mu_{Pt}$$

As can be seen in Table S9 and Table S10, both Nano-QSAR models successfully passed Tropsha's recommended tests for predictive ability.[42, 44] According to Roy *et al.*[61] external predictivity of any QSAR model should be checked by the MAE-based metrics that rely on the predictive error values based on the allowable error limit relatively to the training set response range. The determination of the threshold value for the error values in the external validation (MAE_{EXT}) should be checked by the following criteria: (i) good prediction can be expected if MAE ≤ 0.1x of training set range and MAE + 3σ ≤ 0.2 of training set range; (ii) bad prediction can be expected if MAE > 0.15x of training set range or MAE + 3σ > 0.25 of training set range; (iii) moderate quality if do not fall under either of the described conditions. For developed Nano-QSAR model (Eq. 6) MAE is equal to 0.10, the training range is 1.35, while the MAE + 3σ is 0.55. The best prediction can be expected if MAE ≤ 0.14 and MAE + 3σ ≤ 0.27 and bad prediction can be expected if MAE > 0.20 or MAE + 3σ > 0.34. For the second developed Nano-QSAR model (Eq. 7) MAE is equal to 0.13, the training range is 1.35, while the MAE + 3σ is 0.58. The best prediction can be expected if MAE ≤ 0.14 and MAE + 3σ ≤ 0.27 and bad prediction can be expected if MAE > 0.20 or MAE + 3σ > 0.34. Since in both cases the predictions fulfill the described conditions only in part (0.14 > MAE < 0.20 and 0.27 < MAE + 3σ > 0.34), the prediction can be considered as of moderate quality.

Both developed Nano-$QSAR_{mix}$ models (eq. 6 and eq. 7) explain 93% and 94% of the variability of observed cytotoxicity, respectively. In addition both Nano-$QSAR_{mix}$ models were characterized by the satisfactory goodness-of-fit, the robustness and the external predictive performance (high values of R^2, Q^2_{CV}, R^2_{Ext}, as well as low values of the errors: $RMSE_C$, $RMSE_{CV}$ and $RMSE_P$). Strong linear correlations between the observed and predicted values of $\log(EC_{50})^{-1}$ - graphically presented in Figure 3(a) and 3(b), respectively – proved good fit and high predictive ability both models. Additionally, the plot of standardized cross-validated residuals versus leverages (Williams plot) confirms that all training and validation compounds are located within the applicability domain area i.e., the area defined by structural similarity of the nanoparticles, where the predictions are reliable (SI, Table S7). In addition, the AD has been verified by using basic theory of the standardization approach, as proposed by Roy *et al.*[62] The standardization approach is a simple method for defining the X-outliers (in the case of the training set) and identifying the compounds that reside outside the domain (in the case of the validation set).[62] Obtained results (Table S7 and Table S8) confirmed that there is no outliers and neither of the compounds reside outside the AD. As such, both applied approaches of AD determination (i.e. the leverage approach and the standardization approach) confirmed the reliability of both developed Nano-QSAR models.

In order to alleviate chance correlation, and evaluate the significance of the developed Nano-QSAR model, Y-randomization test (so-called Y-scrambling test) was additionally performed.[63-64] The results of the 5000-fold Y-scrambling test confirmed that both Nano-QSAR models show performance significantly better than those obtained when the descriptors (i.e. $\%mol_{Au}$ and μ_{mix}) were correlated with randomly shuffled values of the cytotoxicity data

(i.e. $\log(EC_{50})^{-1}$). As shown in Figure S1, the values of both R^2Y_{scr} and Q^2Y_{scr} for the "true" Nano-QSAR models are almost ten times as high as those randomly generated. For detailed information on the values of the performance metrics and figures, please refer to the Electronic Supporting Information (Table S10, Figure S1).

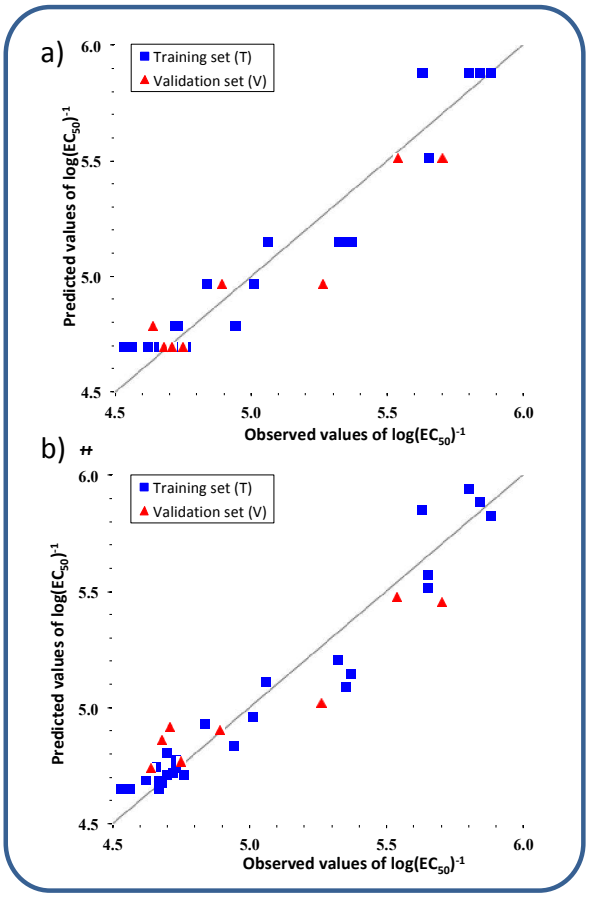

Figure 3. Plot of experimentally determined (observed) versus predicted values of $\log(EC_{50})^{-1}$ with Nano-QSAR$_{mix}$ models eq. 6 and eq. 7, respectively. The diagonal line represents a line of perfect agreement between experimental and calculated values of cytotoxicity.

3.1 Mechanistic interpretation – findings from the Nano-QSAR$_{mix}$ modeling

Both developed Nano-QSAR$_{mix}$ models were analyzed in terms of inducing the potential mechanism(s) of toxicity to the CHO-K1 ovary cell line. In a case of concentration-based Nano-QSAR$_{mix}$ model, represented by Eq. 6, a high linear correlation between the amount of silver metal precursor in a mixture (%mol$_{Ag}$) and the toxicity effect of modified TiO_2-based NPs on the CHO cells simply confirms a well-known fact that increase in concentration of nano-silver leads to increase in the toxicity. Thus, one of the main factor determining toxic effects of silver-containing TiO_2 NPs is the concentration. At the same time, the concentration of nano-silver influence on the amount of Ag^+ ions dissolved in a solution. Since Ag dissolves in water better than other investigated metals (due to the fact that the enthalpy of formation of ion Ag^+ is lower than for other metals), the Ag^+ ion concentration in a solution is higher when comparing an equal mass of other metals and consequently silver species are more available in the solution and therefore more toxic than other metals. This observation is in excellent agreement with literature data.[65-71] It was shown previously that Ag is substantially toxic.[8, 66, 72, 73] Recently, Contreras *et al.*[71] have shown that toxicity of metals to human gingival fibroblast (HGF) decreases in the following order: (most toxic) AgCl>$CuCl_2$>CuCl, $CoCl_2$>$NiCl_2$>$FeCl_2$, $FeCl_3$ (least toxic). The authors confirmed that Ag^+ is the most toxic among various metal cations tested. In addition, they have demonstrated that silver cations are able to induce internucleosomal DNA fragmentation and consequently non-apoptotic cell death.[71] Moreover Li *et al.*[74] have indicated that activated by UV Ag-TiO_2 NPs exhibited stronger bactericidal activity than UV alone, Ag/UV or UV/TiO_2. In addition, for experiments conducted in the dark, bactericidal activity of Ag-TiO_2 nanoparticles was greater than either bare TiO_2 (inert) or pure Ag nanoparticles, suggesting that the hybrid materials produced a synergistic antibacterial effect unrelated to photoactivity.[74]

In a case of mechanistically-based Nano-QSAR$_{mix}$ model, eq. 7, a strong relationship between the absolute electronegativity of the mixture system (μ_{mix}) and the cytotoxicity of Me$_{mix}$@TiO_2 NPs to the CHO ovary cell line was found. An absolute electronegativity expresses the electronic chemical potential and corresponds to the Fermi level, which falls within the middle of the forbidden gap (E_g) region (Figure 4).[74]

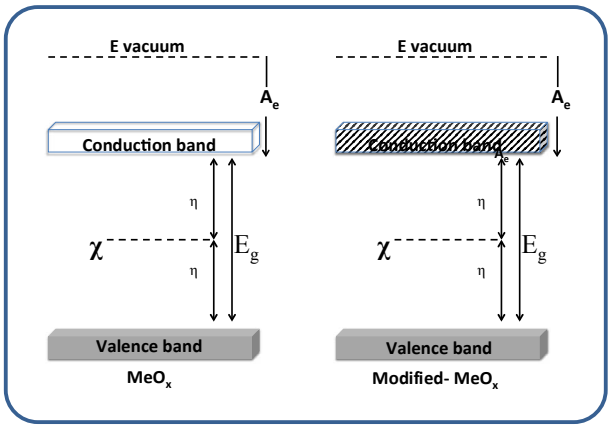

Figure 4. Schematic representation of the band structure of a semiconductors and modified oxide.[74]

According to Portier et al.[72, 76] Mulliken electronegativity (χ) is related to the properties of the cations (eq. 8, Table 1), whereas cation electronegativity (χ_{cation}) mainly depends on the ionic radius (r) and formal charge of the cation (z) (eq. 9).[18, 55]

$$\chi \approx \chi_{cation} + 3.36 \quad (8)$$

$$\chi_{cation} \approx 0.274_z - 0.15_{zr} + 1 + \alpha \quad (9)$$

It is assumed that the highest value of χ_{cation} characterize those cations that have a relatively large charge distributed along a relatively small atomic radius.[18, 55] Thus, χ_{cation} is directly related to detachment of metal cations from the surface of TiO_2. Since electronegativity describes the tendency to attract electrons, it is obvious that the increase of the cation electronegativity should result in increase of the catalytic properties of metal cation and consequently, increase the cytotoxicity of the studied $Me_{mix}@MeO_x$ (i.e. 2nd generation of nanoparticles).[55, 75, 76]

In addition, noble metals on the surface of the TiO_2-based photocatalyst NPs usually play a major role in being the electron donor centers (Fig. 4), and therefore the electron affinity (A_e) might be a main factor responsible for high conductivity of electrons. Since the absolute electronegativity directly correlates with the electron affinity it is expected that the large value of A_e will be accompanied by the large value of μ.[75, 76] A positive value of coefficient (+0.44) for utilized μ_{mix} descriptor (Eq. 7) indicates that increasing value of μ results in higher a toxicity of investigated systems. In other words, the metal cations (i.e. Ag^+) released from the surface of TiO_2 may catalyze the formation of so-called reactive oxygen species (ROS), such as hydroxyl radials ($OH^\bullet$), superoxide anion radicals ($O_2^{\bullet-}$), hydrogen peroxide (H_2O_2).[75, 76] Moreover in the case of considered here TiO_2-based nanomaterials (i.e. $Me_{mix}@TiO_2$), the electron-donor centers that are located on the band-gap (E_g) may absorb the UV or visible light and consequently conduction-band electrons in conduction band and hole (h^+) in the valence band will be photo-generated.[55, 77] Then photo-generated electrons (e^-) can be trapped by noble metals NPs (i.e. Ag) deposited on TiO_2, preventing recombination of the electron-hole pairs on the surface. Generated photo-excited electrons can be transferred to the surface of Ag-containing NPs, instead of losing their recombination activity. This extends the life of the electron-hole pairs, which results in the activity increase and the exhibit high reducing and oxidizing power, respectively. The electrons (e^-) can interact with O_2 and by reduction reaction produce a superoxide anion ($O_2^{\bullet-}$), while the hole (h^+) can generate hydroxyl radicals ($^\bullet OH$) by an oxidative process with water and/or hydroxyl ions (OH^-). In other words, photo-generated holes/electrons promote the ROS generation ($O_2^{\bullet-}$, $^\bullet OH$, $^1O_2$) and consequently damage to the cells is enhanced.[77] In summary, as a result of detachment of Ag from the TiO_2 surface and Ag^+ ion formation, the different types of ROS (e.g. $O_2^{\bullet-}$, $^\bullet OH$, and $^1O_2$) are possibly to be generated. An oxidative stress conducted by ROS is assumed to be the main mechanism of the cytotoxic effect of investigated modified-TiO_2 nanostructures observed in the CHO-K1 ovary cell line.[77] In fact, both descriptors utilized in the final Nano-$QSAR_{mix}$ models (%mol_{Ag} and μ_{mix}) are refer to the same process, i.e. detachment of silver cations from the TiO_2 surface, which determines the cytotoxicity of $Me_{mix}@TiO_2$ NPs to the CHO-K1 ovary cell line (Fig. 5). Positive value of coefficient (+0.44) for utilized μ_{mix} descriptor (eq. 7) indicates that increasing value of μ results in higher toxicity of investigated systems. In the other words the metal cations (i.e. Ag^+) released from the surface of TiO_2 may catalyze the formation of so-called reactive oxygen species (ROS), such as: hydroxyl radials ($OH^\bullet$), superoxide anion radicals ($O_2^{\bullet-}$), hydrogen peroxide (H_2O_2).[54, 59] Moreover in the case of considered here TiO_2-based nanomaterials (i.e. $Me_{mix}@TiO_2$), the electron-donor centers that are located on the band-gap (E_g) may absorb the UV or visible light and consequently conduction-band electrons in conduction band and hole (h^+) in the valence band will be photo-generated.[56, 60, 61] Then photo-generated electrons (e^-) can be trapped by noble metals NPs (i.e. Ag) deposited on TiO_2, preventing recombination of the electron-hole pairs on the surface. Generated photo-excited electrons can be transferred to the surface of Au NPs, instead of losing their recombination activity. This extends the life of the electron-hole pairs, which results in the activity increase and the exhibit high reducing and oxidizing power, respectively. The electrons (e^-) can interact with O_2 and by reduction produce superoxide anion ($O_2^{\bullet-}$), while the hole (h^+) can generate hydroxyl radicals ($^\bullet OH$) by an oxidative process with water and/or hydroxyl ions (OH^-). In the other words photo-generated holes/electrons promotes ROS generation ($O_2^{\bullet-}$, $^\bullet OH$, $^1O_2$) and consequently damage of the cells is enhanced.[61]

3.2 Comparison with the existing models

Some studies have investigated the possibility of QSAR modeling for 2nd generation NPs. Recently, Fourches *et al.*[14] have developed binary classification models for a set of 44 diverse manufactured nanoparticles (MNPs) with different metal cores and surface modifications. However, obtained models that were capable to assign MNPs to one of two distinct classes defined by their biological activity were developed by employing four experimentally measured descriptors only (namely: size, relaxivities (R1 and R2), and zeta potential). In the same paper, the authors have also reported the results of QSAR modeling of pancreatic cancer cells (PaCa2) uptake for 109 superparamagnetic nanoparticles with the same core but different surface modifiers. However, since the structure of organic small molecule conjugated to the MNP surface was the only difference from one MNP to another the authors have provided a set of 150 two-dimensional MOE descriptors calculated for the surface attachments (i.e. conjugated small molecules) only.[14] Two years later, Epa *et al.*[78] have used the same dataset to generate Nano-QSAR model for the cellular uptake of nanoparticles. In addition, the authors have extended the quantitative structure–activity relationship modeling to the second cell line, i.e. human umbilical vein endothelial cell (HUVEC). In order to describe the structural features of studied chemicals a set of 691 molecular descriptors (such as: constitutional, topological, path counts, connectivity indices, information indices, edge adjacency indices, topological charge, eigenvalue-based indices, 2D binary fingerprints) has been calculated. However, similarly to the previous study the authors have developed QSAR models using the descriptors representing molecular species on the nanoparticle surface only, i.e. organic molecules.[71] In light of the foregoing, it is apparent that abovementioned in the introduction section the Nano-QSAR models for 2nd generation NPs don't employ mixture-based descriptors. Therefore, since the idea of additive descriptors for mixture systems accounts for the contributions of each component in a nanoparticle, we have assumed that application of mixture-based

descriptors describes well the unique physicochemical and electronic properties of 2nd generation NPs. According to our best knowledge, the proposed approach is the first attempt to use mixture-based descriptors in the Nano-QSAR modeling of 2nd generation NPs.

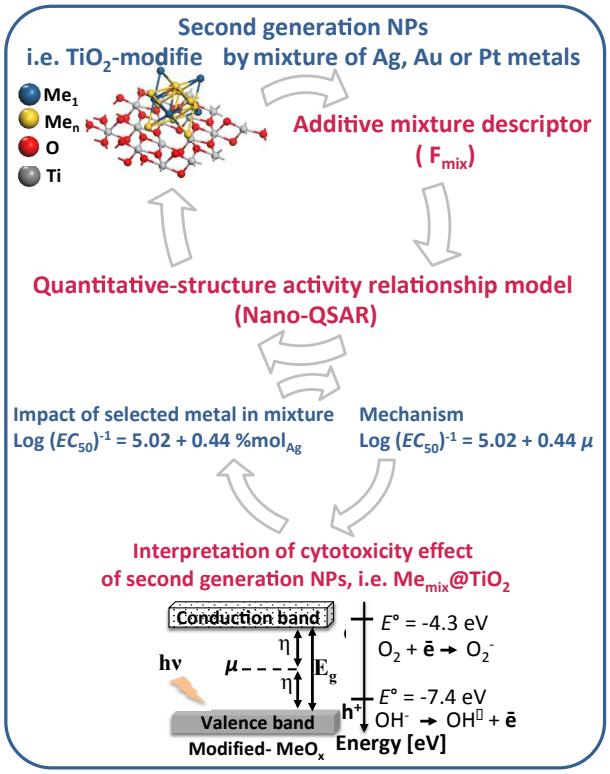

Figure 5. The scheme of probable mechanism of toxicity – findings from the Nano-QSAR$_{mix}$ analysis (concentration-based cytotoxicity model (eq. 6) and mechanistically-based cytotoxicity model (eq. 7)).

4. Conclusions

Propose approach is the first published example of the use of additive mixture-based descriptors to characterize and encode the structure of the 2nd generation NPs. A great advantage of presented approach is the fact that it allows to describe the properties of 2nd generation NPs taking into account various modifications such as: a variety of concentrations of single metal cluster, different type and amount of noble-metal precursor on the surface of TiO_2-based NPs. In addition, the usefulness and the effectiveness of the proposed approach for calculating the additive descriptors for 2nd generation NPs has been proven by development of interpretative Nano-QSAR models describing the cytotoxicity of 34 MeO_x TiO_2 NPs. Thereby, in the light of the results obtained, the proposed approach may have a significant practical aspects. Thus, this approach may be used for the following: (1) to describe the structure and properties of 2nd generation NPs and, (2) as an efficient tool to predict the toxicity as well as physicochemical properties of unexplored 2nd generation NPs.

Conflicts of interest

The authors declare no competing financial interest.

Acknowledgements

This material is based on research sponsored by the *European Commission through Marie Curie IRSES* program, *NanoBRIDGES project* (FP7-PEOPLE-2011-IRSES, Grant Agreement Number 295128). A.M. thanks the *National Science Center* (no. 2015/19/N/NZ7/01593) for financial support. A.G. thanks L'Oréal-UNESCO for granting her a For Women in Science 2017 Fellowship. B.R. gratefully acknowledges support from the North Dakota State University Center for Computationally Assisted Science and Technology and the U.S. Department of Energy through Grant No. DE-SC0001717.

Author Contributions

A.G, T.P, A.Z-M supervised and directed the project. A.M performed quantum-mechanical calculations, developed and validated the Nano-QSAR models, analysed experimental data and results; A.M, A.G, B.R discussed the results and wrote the manuscript; E.M. designed and performed experimental research on cytotoxicity, processed experimental data; M.M, M.D, S.H designed and performed 2nd generation NPs synthesis. All authors have given approval to the final version of the manuscript.

References

1 The Global Market for Metal Oxide Nanoparticles 2016-2020, Report, Dublin, Ireland, 2016.
2 A. Mikolajczyk, A. Malankowska, G. Nowaczyk, A. Gajewicz, S. Hirano, S. Jurga, A. Zaleska-Medynska and T. Puzyn, *Environmental Science: Nano*, 2016, **3**, 1425-1435.
3 N. Serpone and A.V. Emeline, *The journal of physical chemistry letters*, 2012, 3, 673-677.
4 X. Chen and S. S. Mao, *Chemical reviews*, 2007, 107, 2891-2959.
5 R. D. Handy, R. Owen and E. Valsami-Jones, *Ecotoxicology*, 2008, **17**, 315-25.
6 R. D. Handy, F. Von der Kammer, J. R. Lead, M. Hassellöv, R. Owen and M. Crane, *Ecotoxicology*, 2008, **17**, 287-314.
7 E. Valsami-Jones and I. Lynch, *Science*, 2015, **350**, 388-389.
8 J. C. Dearden *International Journal of Quantitative Structure-Property*, 2016, **1**, 1-14.
9 K. Roy, P. Ambure, S. Kar and P. K. Ojha, *Journal of Chemometrics*, 2018, **159**, 1-18.
10. H. Zhu, T. M. Martin, L. Ye, A. Sedykh, D. M. Youn and A. Tropsha. Chemical Research in Toxicology, 2009, **22**,1913-1921.
11 T. Puzyn, B. Rasulev, A. Gajewicz, X. Hu, T. P. Dasari, A. Michalkova, H. M. Hwang, A. Toropov, D. Leszczynska and J. Leszczynski, *Nature Nanotechnology*, 2011, **6**, 175-178.
12 T. Puzyn, D. Leszczynska and J. Leszczynski, J *Small*, 2009, **5**, 2494-2509.11. Todeschini R.; Consonni, V. Handbook of Molecular Descriptors. Wiley-VCH Verlag GmbH, 2000.

13 D. A. Winkler, M. Breedon, A. E. Hughes, F. R. Burden, A. S. Barnard, T. G. Harvey and I. Cole, *Green Chemistry*, 2014, **16**, 3349-3357.
14 L. Zhang, P. J. Zhou, F. Yang and Z. D. Wang, *Chemosphere*, 2007, **67**, 396-401.
15 D. Fourches, D. Pu, C. Tassa, R. Weissleder, S. Y. Shaw, R. J. Mumper and A. Tropsha, *ACS Nano*, 2010, **4**, 5703-5712.
16 R. Liu, H. H. Liu, Z. Ji, C. H. Chang, T. Xia, A. E. Nel, and Y. Cohen, *ACS Nano*, 2015, **9**, 9303-9313.
17 R. Liu, R. S. Rallo, S. George, Z. Ji, S. Nair, A. E. Nel and Y. Cohen, *Small*, 2011, **7**, 1118-1126.
18 V. C. Epa, F. R. Burden, C. Tassa, R. Weissleder, S. Shaw and D. A. Winkler, D,*Nano Letter*, 2012, **12**, 5808-5812.
19 A. Gajewicz, N. Schaeublin, B. Rasulev, S. Hussain, D. Leszczynska, T. Puzyn and J. Leszczynski, *Nanotoxicology*, 2014, **9**, 1-13.
12 A. Mikolajczyk, A. Gajewicz, B. Rasulev, N. Schaeublin, E. Maurer-Gardner, S. Hussain, J. Leszczynski and T. Puzyn, *Chemistry of Materials*, 2015, **27**, 2400-2407.
21 S. Kar, A. Gajewicz, T. Puzyn and K. Roy, *Toxicology in Vitro*, 2014, **28**, 600-606.
22 S. Kar, A. Gajewicz, T. Puzyn, K. Roy and J. Leszczynski, *Ecotoxicology Environmental Safe*, 2014, **107**, 162-169.
23 A. Mikolajczyk, H. P. Pinto, A. Gajewicz, T. Puzyn and J. Leszczynski, *Current Topics in Medicinal Chemistry*, 2015, **15**, 1859-1867.
24 K. Jagiello, B. Chomicz, A. Avramopoulos, A. Gajewicz, A. Mikolajczyk, P. Bonifassi, M. G. Papadopoulos, J. Leszczynski and T. Puzyn, *Structural Chemistry*, 2017, **28**, 635-643.
25 A. Mikolajczyk, N. Sizochenko, E. Mulkiewicz, A. Malankowska, M. Nischk, P. Jurczak, S. Hirano, G. Nowaczyk, A. Zaleska-Medynska, J. Leszczynski, A. Gajewicz and T. Puzyn, *Beilstein Journal of Nanotechnology*, 2017, **8**, 2171-2180.
26 N. Sizochenko, A. Gajewicz, J. Leszczynski, and T. Puzyn, *Nanoscale*, 2016, **8**, 7203-7208.
27 N. Sizochenko, B. Rasulev, A. Gajewicz, V. Kuz'min, T. Puzyn and J. Leszczynski, *Nanoscale*, 2014, **6**, 13986-13993.
28 N. Sizochenko, A. Mikolajczyk, K. Jagiello, T. Puzyn, J. Leszczynski and B. Rasulev, *Nanoscale*, 2017, **10**, 582-591
29 E. Wyrzykowska, A. Mikolajczyk, C. Sikorska and T. Puzyn, *Nanotechnology*, 2016, **27**, 445702.
30 E. Burello, A. P. Worth, *Nanotoxicology*, 2011, **5**, 228-235.
31 J. Hermens and P. Leeuwangh, *Ecotoxicology Environmental Safty*, 1982, **6**, 302-310.
32 N. Nirmalakhandan, E. Egemen, C. Trevizo and S. Xu, *Ecotoxicololgy Environmental Safety*, 1998, **39**, 112-119.
33 M. C. Berenbaum, *Theoretical Biology*, 1985, **114**, 413-431.
34 R. L. Plackett and P. S. Hewlett, *Biometrics*, 1967, **23**, 27-44
35 E. N. Muratov, E. V. Varlamova, A. G. Artemenko, P. G. Polishchuk and V. E. Kuz'min, Mixtures *Molecular Informatics,* 2012, **31**, 202-221.
36 M. Junghans, T. Backhaus, M. Faust, M. Scholze and L. H., *Aquatic Toxicology,* 2006, **76**, 93-110.
37 L. S. McCarty, G. W. Ozburn, A. D. Smit and D.G. Dixon, *Environmental Toxicology Chemistry*, 1992, **11**, 1037-1047.
38 P. S. Hewlett and C. F. Wilkinson, *Journal of the Science of Food and Agriculture*, 1967, **18**, 279.
39 R. Altenburger, H. Walter and M. Grote, *Environmental Science and Technology,* 2004*,* **38**, 6353-6362.
40 L. Zhang, P. J Zhou, F. Yang, and Z. D. Wang, *Chemosphere*, 2007, *67*, 396-401.
41 S. Xu and N. Nirmalakhandan, *Water Research*, 1998, **32**, 2391-2399.
42. A. Golbraikh and A. Tropsha, *Journal of Molecular Graphics and Modelling*, 2002, **20**, 269-276.
43. G. Melagraki and A. Afantitis, *RSC Advances,* 2014, **4**, 50713-50725.
44. A. Tropsha, *Molecular Informatics*, 2010, **29**, 476–488
45. K. Roy and P. Ambure, *Chemometrics and Intelligent Laboratory Systems*, 2016, **159**, 108-126
46 D. L. Wang, Y. Gao, Z. F. Lin, Z. F. Yao and W. X. Zhang, *Aquatic Toxicology*, 2014, **154**, 200-206.
47 C. Wang, G.H. Lu, Z. Y. Tang and X. L. Guo, *Journal of Environmental Sciences* , 2008, **20**, 115-119.
48 R. Todeschini, and V. Consonni, *Molecular Descriptors for Chemoinformatics,* 2009*,* **41**, John Wiley & Sons.
49 M. J. Frisch, T. G. Schlegel, G. E. Scuseria, M. A. Robb, J. R. Cheeseman, G. Scalmani, V. Barone, B. Mennucci, G. A. Petersson, H. Nakatsuji, M. Caricato, X. Li , F.P. Hratchian, A. F. Izmaylov, J. Bloino, G. Zheng, J. L. Sonnenberg, M. Hada, M. Ehara, K. Toyota, R. Fukuda, J. Hasegawa, M. Ishida, T.; Nakajima, Y. Honda, O. Kitao, H. Nakai, T. Vreven, J. A. Montgomery, J. E. Peralta, F. Ogliaro, M. J. Bearpark, J. Heyd, E. N. Brother, K. N. Kudin, V. N. Staroverov, R. Kobayashi, J. Normand, K. Raghavachari, A. P. Rendell, J. C. Burant, S. S. Iyengar, J. Tomasi, M. Cossi, N. Rega, N. J. Millam, M. Klene, J. E. Knox, J. B.; Cross, V. Bakken, C. Adamo, J. Jaramillo, R. Gomperts, R. E. Stratmann, O. Yazyev, A. J. Austin, R. Cammi, C. Pomelli, J. W. Ochterski, R. L. Martin, K. Morokuma, V. G. Zakrzewski, G. A. Voth, P. Salvador, J. J. Dannenberg, S. Dapprich, A. D. Daniels, J. B. Foresman, J. V. Ortiz, J. Cioslowski and D. J. Fox, Gaussian 09, Gaussian, Inc. 2009, Wallingford, CT, USA.
50 S. Ikalainen, S. and K. Laasonen, *Physical Chemistry Chemical Physics,* 2013, **15**, 11673-11678.
51 J. K. Perdew, B. Kieron and M. Ernzerhof, *PhysIcal Review Letter,* 1996, **77**, 3865-3868.
52 G. Kresse and J. Furthmüller, *Computational Material Science,* 1996, **6**, 15-50.
53 G. Kresse and D. Joubert, *Physical Review B*, 1999, **59**, 1758-1775.
54 E. Finazzi, C. Di Valentin, G. Pacchioni and A. Selloni, *The Journal of Chemical Physics,* 2008, **129**, 154113.
55 R. G. Pearson, *Inorganic Chemistry,* 1988, **27**, 734-740.
56 T. Puzyn, A. Mostrag-Szlichtyng, A. Gajewicz, M. Skrzynski and A. P. Worth, *Structural Chemistry,* 2011, **22**, 795-804.
57 J. Devillers, J., *Genetic algorithms in molecular modeling*. Academic Press, 1996.
58. OECD Document, Guidance Document on the Validation of (Quantitative) 1226 Structure–Activity Relationships (Q)SARs Models, ENV/JM/MONO(2007) 2. 2007.
59 N. Chirico, N. and P. Gramatica, *Journal of Chemical Informatics and Modelling,* 2011, **51**, 2320-2335.
60 P. Gramatica, *QSAR & Combinatorial Science,* 2007, **26**, 694-701.
61 K. Roy, S. Kar and P. Ambure, *Chemometrics and Intelligent Laboratory Systems,* 2015, ***145***, 22-29.
62 K. Roy, N. R. Das, P. Ambure and N. B. Aher, *Chemometrics and Intelligent Laboratory Systems,* 2016, **152**, 18-33.
63. S. Zhang, A. Golbraikh, S. Oloff, H. Kohn and A. Tropsha *Journal of Molecular Graphics and Modelling*, 2006, **46**, 1984-1995.
64. G. Melagraki and A. Afantitis, *Current Topics in Medicinal Chemistry,* 2015, **15**, 1827-1836.
65 R. Asahi, T. Morikawa, T. Ohwaki, K. Aoki and Y. Taga, *Science*, 2001, **293**, 269-271.
66 P. V. Asharani, M. P. Hande and S. Valiyaveettil, *Abstract of Papaper of American Chemistry Society,* 2008, ***236***.
67 V. De Matteis, M. A Malvindi, M. A.; Galeone, A.; Brunetti, V.; De Luca, E.; Kote, S.; Kshirsagar, P.; Sabella, S.; Bardi, G.; Pompa, P. P. *Toxicolology In Vitro*, 2016, *37*, 201-210.

68 V. De Matteis, M. A. Malvindi, A. Galeone, V. Brunetti, E. De Luca, S. Kote, P. Kshirsagar, S. Sabella, G. Bardi and P. P. Pompa, *Nanomedicine: NBM*, 2015, **11**, 731-739.
69 A. Katsumiti, D. Gilliland, I. Arostegui and M. P. Cajaraville, *Plos One,* 2015*,* **9**, 543-553.
70 M. M. Seitkalieva, A.S. Kashin, K. S. Egorova and V.P. Ananikov, *ACS Sustainable ChemIstry & Engineering*, 2017.
71 Contreras, R. G.; Sakagami, H.; Nakajima, H.; and J. Shimada, *In Vivo,* 2010, **24**, 513-517.
72 K. Kawata, M. Osawa and S. Okabe, *Environmental Science & Technology,* 2009, **43**, 6046-6051.
73 A. R. Gliga, S. Skoglund, I. O. Wallinder, B. Fadeel and H. L. Karlsson, *Particle and Fibre Toxicology*, 2014, **11**, 1-17.
74 M. Li, M. E. Noriega-Trevino, N. Nino-Martinez, C. Marambio-Jones, J. Wang, R. Damoiseaux, F. Ruiz and E. M. Hoek, *Abstract Paper of Am. Chem. S.* 2011, *241*, 8989-8995.
75 J. Portier, G. Campet, C. W. Kwon, J. Etourneau and M. A. Subramanian, *International Journal of Inorganic Materials,* 2001, **3**, 1091-1094.
76 J. Portier, G. Campet, A. Poquet, C. Marcel and M. A. Subramanian, *International Journal of Inorganic Materials,* 2001, **3**, 1039-1043.
77 Y. Li, W. Zhang, J. Niu, Y. Chen, *ACS Nano,* **2012**, **6**, 5164-5173.
78 V. C. Epa, F. R. Burden, C. Tassa, R. Weissleder, S. Shaw and D. A. Winkler, *Nano Letter*, 2012, **12**, 5808-5812.

Graphical Abstract